

RESEARCH ARTICLE

Combined loading performance analysis of gasketed bolted flange joints with emphasis on bolt scattering

K.A. Khan*, I. Ahmed

 Department of Mechanical Engineering, Pakistan Institute of Engineering & Applied Sciences, Nilore, 45650, Islamabad, Pakistan
 Phone: +92 51 9248611; Fax: +92 51 9248600

ABSTRACT - Gasketed bolted flange joints (GBFJ) are commonly used in various industries however, their failure could result in significant losses not only in terms of financial but human life as well. Most of the work present on the performance of the GBFJ involves simplified assumptions by neglecting the effect of bolt scatter. Also, there is a paucity of studies investigating the sealing performance of GBFJ under combined thermal transient and structural loading. In the present study, two different flange sizes of ANSI B16.5 pressure class 900 (4in. and 6in.) are evaluated, using a detailed three-dimensional finite element analysis (FEA). ASME bolt tightening scheme was applied for the preloading of the bolts. Higher bolts and gasket stresses were observed in the case of 6in. flange joint. Also, greater variation in bolt stresses (up to 18 % of the target value) was observed for the 6 in. model which may be due to higher number of bolts resulting in greater scattering phenomena. Both models were found to be safe under the structural loading. However, large relaxation in stresses was observed at high bulk temperature. The gasket stress in 4in. flange model was observed to be less than the minimum seating stress (69 MPa) at temperatures greater than 300 °C implying possible leakage. However, stresses in the 6in. model stayed within the safe limit throughout the thermal and structural loading due to higher bolt target stresses, resulting in its proper seating even at higher temperatures.

ARTICLE HISTORY
 Received : 07th Feb. 2023
 Revised : 13th July 2023
 Accepted : 04th Aug. 2023
 Published : 28th Sept. 2023
KEYWORDS
Bolted joint
Flange
FEA
Leakage
Thermal transient

1.0 INTRODUCTION

Bolted flange joints are a critical component of pressure vessels and piping networks. Due to their design simplicity and ease of assembly/disassembly methods, they represent a flexible option for fastening pipes and other equipment. However, failure of the bolted joints due to structural and or leakage issues is one of the major problems faced regarding their usage in the industries. Substantial research has already been done to assess the leakage performance of the joint. However, most of the research work present in literature either uses a two-dimensional or a three-dimensional axisymmetric model which greatly simplifies the model ignoring some important factors like bolt scattering. Similarly, minimal work is present regarding the effects of transient thermal loading. The effect of temperature on the flange joint has also not been discussed in the design codes. Analytical studies have been done to evaluate the stress variation through different parts of the joint during assembly and operation [1-4] Several studies have been done to include the non-linear behaviour of the gasket material during the loading and unloading process [5, 6]. Stress variation in gasketed and non-gasketed flange joints have also been compared using numerical analysis as well as through experimental study [7, 8]. The effects of different bolt tightening strategies on the strength of the joint have been discussed without the application of internal pressure [9] as well as under the joined action of pressure and axial load [10]. The impact of bending load and internal pressure on the joint integrity has also been studied with axial loading [11] as well as without axial loading for both single and double gasket joints [12].

In nuclear power plants and petrochemical industries, the BFJ is subjected to high-temperature fluids which may result in leakage of the joint. This is because when BFJ is subjected to high temperature, expansion of the joint takes place which causes relaxation of the joint resulting in possible loss of gasket contact stress. A few studies [13-15] have also been carried out to determine the impact of temperature on the joint. The behaviour of the GBFJ under the action of internal pressure and thermal steady-state loading has been discussed using two different types of gaskets [13]. Steady state assumption does not provide an accurate analysis as the thermal loading is actually transient in nature. Gasket sealing capability is considerably affected by the heating rate which is ignored in the steady state analysis. The variation of flange stress due to transient thermal loading has also been discussed by performing a three-dimensional axisymmetric analysis [14]. The effect of temperature on gasket relaxation for both single and double gasket joints has also been studied [15].

Thus, in the current study, a three-dimensional evaluation of the GBFJ is done under the joined action of structural and transient thermal loading while incorporating bolt scattering phenomena. The evaluation is done on two different flange sizes to compare their working under the combined loading.

2.0 METHODS AND MATERIALS

An overview of the methodology employed for the present study is shown in Figure 1.

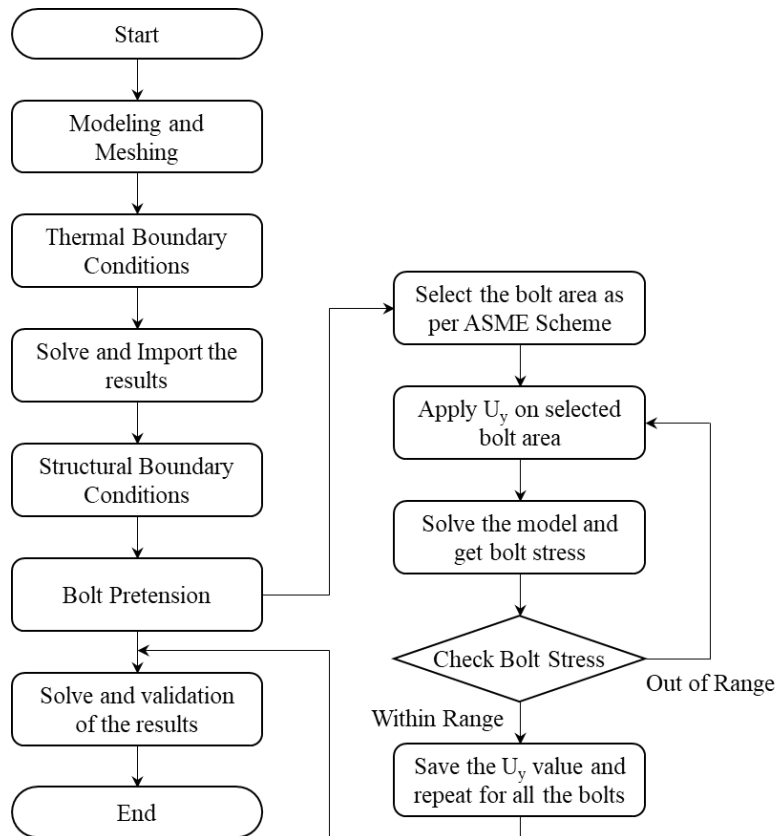


Figure 1. FEA methodology

2.1 Geometric Modelling

A three-dimensional model of the flange joint is created for both sizes using general purpose finite element software. A 4 in. and 6 in. Nominal Pipe Size (NPS) flanges of pressure class 900 along with spiral wound gasket are chosen for this study. ANSI B16.5 standard dimensions are followed for modelling of both flange sizes [16]. For gasket, only the sealing element is modelled as this plays a fundamental part towards its sealing capability. Symmetry is considered across the gasket mid-plane and only single side of the BFJ is modelled in each case. Figure 2 shows the complete assembled model for 6in. flange.

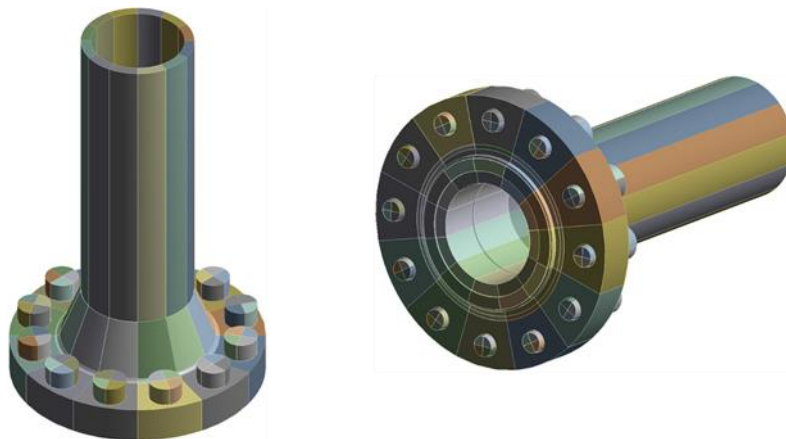


Figure 2. Complete assembled model of the 6in. BFJ

The selection of material for different components of BFJ is done based on the past work available in the literature [13]. For pipe and flange, ASTM 350 LF2 material is used. For bolts, ASTM SA 193 B7 material is chosen. The spiral wound gasket is selected for the current study which is made by winding strips of metal and a soft fiber sealing material under pressure. The material used for the gasket is ASTM A 182. For accurate simulations, temperature-dependent material properties are considered for the current study. All the properties of the materials are taken as per ASME Boiler and Pressure Vessel Code [17]. To model the plastic behaviour of flange and bolts, the bilinear kinematic hardening

model is also defined which contains two parts each having different slopes to define the behaviour of the material completely. The first slope defines the elastic behaviour of the material up to yield strength. The second slope, having tangent modulus as the gradient, defines the plastic behaviour of the material after the yield strength. For current study, the tangent modulus is taken as 10% of Young's modulus [18]. To incorporate gasket non-linearity, the spiral wound gasket stress-strain relationships presented by Fukuoka et al. [3] are used. Two different elastic moduli are used for the loading and unloading of the gasket. These loading and unloading curves are input into the FE model to simulate gasket non-linear behaviour.

2.2 Meshing

Before performing FEA analysis, a higher quality mesh of the geometric model is required. For this purpose, the model is sliced into various parts to get hexahedral mesh. Finer mesh is created in critical regions like gasket body, flange hub fillet, and contact areas. The meshing of flange, bolt, and gasket is given in Figure 3.

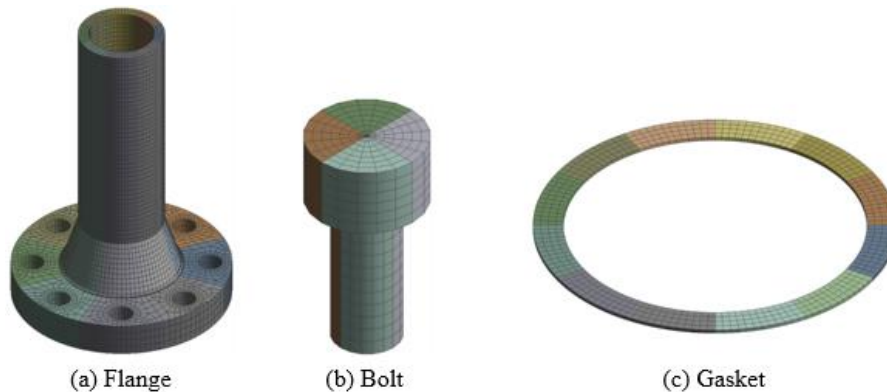


Figure 3. Meshing of flange, bolt, and gasket

To model the interaction between various components of the BFJ, contact regions are defined between different mating surfaces of the model. The main purpose of defining contacts is to prevent two mating surfaces from penetrating each other. Here three pairs of contact regions are defined. These include contact between the bottom face of bolt heads and flange top face, contact between gasket top face and flange raised face, and contact between bolt shanks and flange holes. All three contact pairs are modelled as frictionless. SOLID185 and SOLID70 elements are used to mesh the model for structural and thermal analysis respectively. The gasket is meshed using INTER195 element to model the deformation of the gasket in the through-thickness direction. Similarly, CONTA174 and TARGE170 elements are used to for the contact and target surfaces respectively in the contact regions.

2.3 Boundary Conditions

Transient analysis is considered for thermal loading as it helps us to simulate actual loading conditions. Initially, at the start ($t = 0$), the model is assumed to be at room temperature (20 °C). For thermal analysis, convection at the internal and external surfaces of the BFJ is considered. At the internal surface, convection is considered with the bulk fluid temperature of 100 °C and at the external surface, convection at 20 °C is considered. The internal thermal coefficient is set to 150 W/m²-°C and the external coefficient is considered to be 20 W/m²-°C [19]. The model is then solved for 1600 seconds so that steady-state is achieved. After solving for 100 °C, the bulk fluid temperature is varied to 200 °C - 400 °C, and the model is solved each time to study the temperature distribution across BFJ at different bulk temperatures. The same process is then repeated for the 6in. flange size as well.

The flange is neither axially nor radially constrained which helps us to capture rotation of the flange. However, the bolts are restricted both radially and tangentially by applying nodal constraints to the midplane of bottom of each shank. This is done to observe the bolt bending behaviour. Symmetry is employed to the lower face of the gasket body. Contact initialization is done between bolts and flange by applying a small nodal displacement (U_y) value to the bottom face of each shank. This mirrors the hand tightening of the bolts in real life. Next, bolt pretensioning is done by tightening the bolts to the target stress value. For this purpose, torque control method is used along with ASME guidelines as explained in the next section. After the completion of bolt tightening process, pressure is applied to the internal of the BFJ. In the present study, an internal pressure of magnitude 15.3 MPa is applied to the inner of both joints [6]. Due to the applied pressure, a resulting axial force also acts upon the pipe. This is applied as a nodal pressure at the end of the pipe [20]. Its magnitude is set to 23.1 MPa for the 4in. flange and 34 MPa for the 6in. flange. A summary of all the boundary conditions (both thermal and structural) is shown in Figure 4.

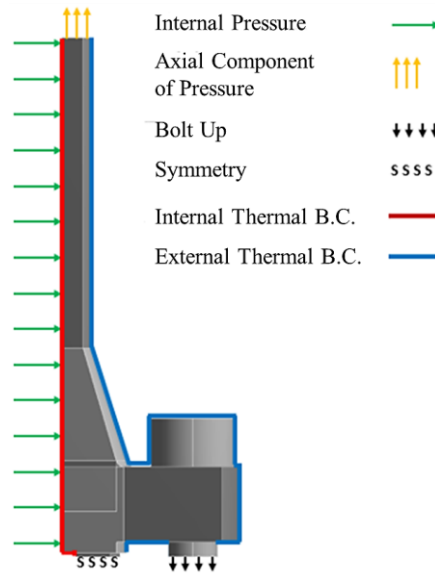


Figure 4. Boundary conditions

2.4 Bolt Preloading

The bolts are preloaded by using the torque control method in which each bolt is loaded individually to the target torque value. ASME tightening scheme [21] is adopted in the present study to tighten the bolts to the target value as it is proved to be more suitable in sealing the joint as compared to industrial strategy [9]. ASME scheme consists of four passes to tighten the bolts to the target value. In the first three passes, the bolts are tightened in a cross pattern while in the final pass, bolts are preloaded in a clockwise pattern. The cross sequence for 4in. (1, 5, 3, 7, 2, 6, 4, 8) and 6 in. flange (1, 7, 4, 10, 2, 8, 5, 11, 3, 9, 6, 12) is shown in Figure 5.

In the current study, target torque for the case of 4in. flange is 700 Nm [8]. Similarly, for 6in. flange the target torque is 900 Nm [22]. The target stress corresponding to the torque value is calculated using Eq. 1 and Eq. 2. The corresponding target torque and stress value for each tightening pass is given in Table 1. During the analysis, bolt preloading is accomplished by applying a displacement ‘ U_y ’ value at the bottom face of the bolt shank, then checking the ensuing stress and repeating this process until the resulting stress meets the target value. The same process is followed for each bolt and all the bolts are tightened to the required stress.

$$T_b = F_b (KD_b) \tag{1}$$

$$\sigma_b = \frac{F_b}{A_b} \tag{2}$$

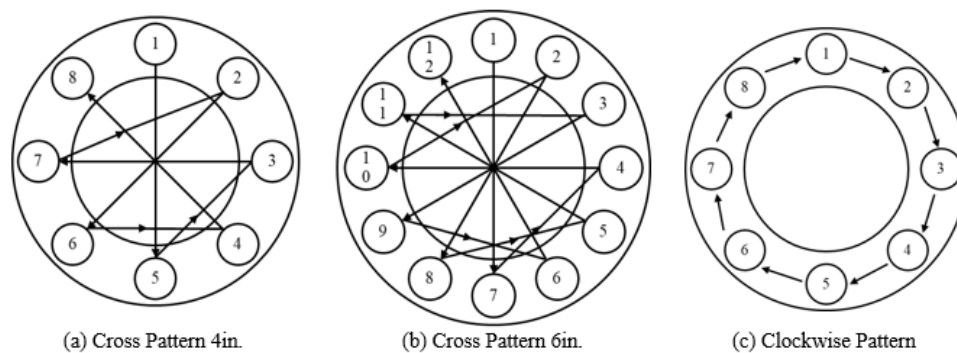


Figure 5. Bolt tightening sequences

Table 1. Bolt target stress for both flange sizes

Flange Size	Pass No.	Target Torque (%)	Applied Torque (Nm)	Bolt Load (kN)	Target Stress (MPa)	Tightening Pattern
4in.	1	20-30	140	24.5	38.2	Star
	2	50-70	420	73.5	114.5	Star
	3	100	700	122.5	191	Star
	4	100	700	122.5	191	Clockwise
6in.	1	20-30	180	31.5	49	Star
	2	50-70	540	94.5	147.25	Star
	3	100	900	157.5	245.5	Star
	4	100	900	157.5	245.5	Clockwise

2.5 FE Model Validation

The results of the thermal analysis are verified analytically using equivalent thermal resistance model [23]. A very small difference is observed between the FEA and theoretical results when the bulk fluid temperature is varied from 100-400 °C as shown in Table 2 and Figure 6(b) for the case of 4in. flange. The thermal analysis results are in good agreement with the results reported in the literature [24]. Similar trend is also observed in 6in. flange model, thus validating our transient thermal model.

For structural analysis, model is validated by performing theoretical calculations only on the pipe component of both the flanges using Lamé's theory of thick cylinders [20]. A comparison of these FEA and theoretical results is presented in Table 3 which shows a close agreement between both the results, thus verifying our structural analysis as well. Temperature distribution through different components of 4in. BFJ model, for the case of 100 °C bulk temperature, is shown in Figure 6(a). Maximum temperature is observed in the pipe section of the joint which was expected since it is in direct contact with the hot fluid. Similarly, the minimum temperature is observed in the bolts part of the joint as there is no direct heat transfer between the bolts and the hot fluid. The only heat that is transferred to the bolts is through the contact area between bolt heads and flange face. The temperature in the gasket decreases towards the outer diameter and the maximum temperature is observed on the inside diameter as it is directly exposed to the hot fluid. Same trend is seen for all the temperature cases in both BFJ models.

Table 2. Comparison of FEA and theoretical results of thermal analysis (4 in. flange @100 °C)

Sr. No.	Analysis	Pipe Inner	Pipe Outer
		Temperature (°C)	Temperature (°C)
1	FEA	87.359	86.902
2	Theoretical	88.175	87.732
3	Difference	0.925%	0.95%

3.0 RESULTS AND DISCUSSION

During the bolt tightening process, relaxation in bolts occurs due to the elastic interaction between different components of the BFJ which is known as bolt scattering phenomena [21]. The change in bolt 1 stress during pass 1 when all the bolts are tightened is shown in Figure 7(a) for 4in. model. Initially, bolt 1 is tightened to the target stress (38 MPa) value. Then the next bolt (bolt 5) in the sequence is tightened, however, due to the elastic interaction, an increase in stress in bolt 1 is also observed since it is positioned across bolt 5. Similarly, when the next bolt (bolt 3) in the sequence is tightened, a decrease in stress is observed for bolt 1 since it is positioned near bolt 3. Thus, whenever a bolt in the neighbourhood of bolt 1 is tightened, bolt 1 stress is observed to decrease and whenever a bolt that is positioned across bolt 1 is tightened, an increase in its stress is seen. Finally at the end of first pass, after tightening the last bolt (bolt 8), around 80% of the stress in bolt 1 is found to be lost due to the scattering effect. Similar variation in the stress of bolt 1 for the case of 6in flange is also observed as given in Figure 7(b). For 6in. flange, at the end of pass 1 nearly all the stress in bolt 1 is found to be lost and it is observed to be completely relaxed due to the scattering phenomena. This greater stress variation in bolt 1 in case of 6in. flange may be down to the higher number of bolts that are to be tightened after tightening of bolt 1, thus resulting in greater scattering phenomena.

Table 3. Comparison of FEA and theoretical results of structural analysis

Flange Size (NPS)	Analysis	Tangential Stress (MPa)	Radial Stress (MPa)
4in.	FEA	43.042	-13.069
	Theoretical	42.85	-15.3
	Difference	-0.192	-2.231
6in.	FEA	68.662	-13.9
	Theoretical	67.98	-15.3
	Difference	-0.68	-1.4

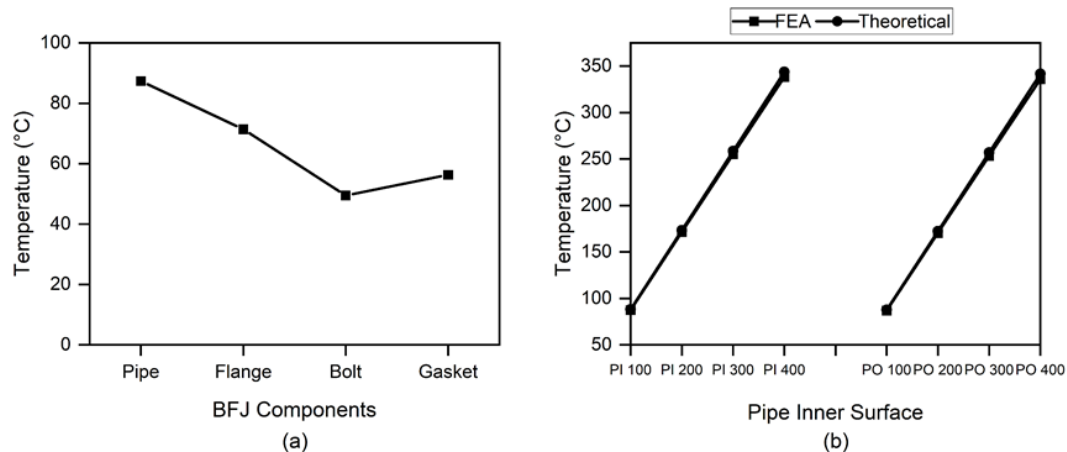


Figure 6. (a) Temperature distribution in BFJ (4 in.) and (b) Comparison of FEA and theoretical results for thermal analysis (4 in.)

To study the bending behaviour of bolts, four nodes are taken along the lower face of the bolt shank at 90° apart from each other as shown in Figure 8(a). Node 1/1 represents the inner node of bolt 1 with respect to the flange internal surface and node 1/2 represents the outer node. While nodes 1/3 and 1/4 represent the side nodes of bolt 1. Similar nomenclature is followed for other bolts of both the flanges. Axial bolt stress is determined at each of these nodes after each tightening round as shown in Figure 9 and Figure 10.

Figure 9 shows that for 4in. flange there is a significant difference in the bolt axial stress in the inner and outer nodes showing the bending of the bolts along that direction. However, in the side nodes, the axial bolt stress is close to each other implying little or no bending along that direction. In bolts 2 and 6, no bending is observed along the side nodes. However, in the remaining bolts, some difference in axial stress is observed, implying bending of the bolts along that direction. The inner nodes located on each bolt exhibit maximum stress while the outer nodes show minimum stress implying bending of the bolt in the outward direction. The inner nodes show maximum stress because, when displacement is applied on the shank, the bolts come into contact with the flange due to deformation. This interaction results in higher stress on the inner nodes of the bolts. A maximum stress of 290 MPa is observed in the inner node of bolt 2 after the 3rd pass. Compressive stresses are also observed in the case of bolt 5 which disappear after 2nd pass of the tightening sequence.

Similarly in the case of 6in flange size, as shown in Figure 10, the stress in the side nodes is close to each other showing little or no bending along that direction. However, the stress in the inner and outer nodes is different implying bolt bending along that direction. This stress difference is observed to get larger with the increasing stress in each pass. Compressive stresses are also seen in bolts 1, 4, and 7 which disappear after the second pass of the tightening sequence. Gasket stress is also determined to verify that it is higher than the minimum seating stress and lesser than the yield strength of the material. This helps us to make sure that the gasket is safe and properly seated and the BFJ is leak-proof. The minimum seating stress for spiral wound gasket is 69 MPa and the yield limit of the gasket is 206 MPa [25]. To determine the variation of gasket stress in case of 4in. flange, eight nodes are taken along the inner as well as the outer diameter of the gasket corresponding to each of the bolt locations as shown in Figure 8(b). Gasket normal stress is then determined at each of these nodes after each pass of tightening sequence. Same procedure is followed for 6in. flange as well, where twelve nodes are taken along the inner and outer diameter.

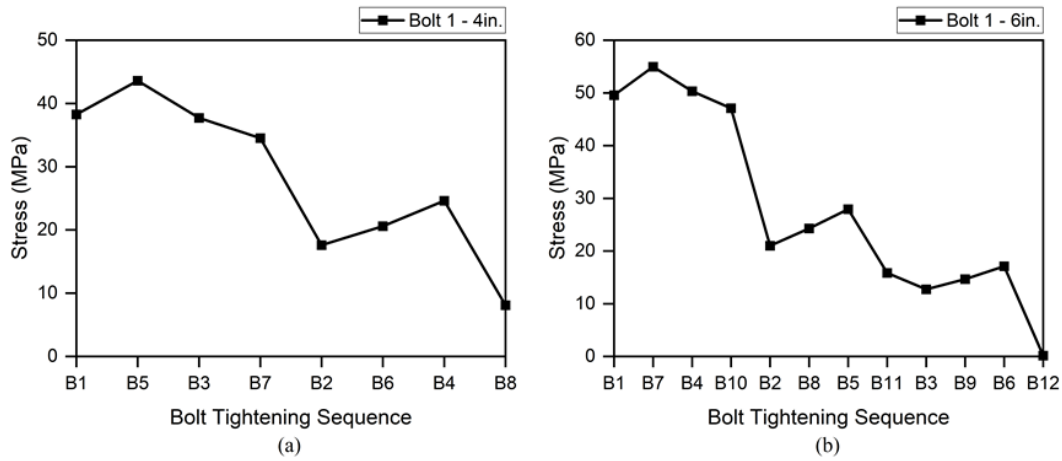


Figure 7. (a) Stress variation in bolt 1 during pass 1 for 4 in. flange and (b) Stress variation in bolt 1 during pass 1 for 6 in. flange

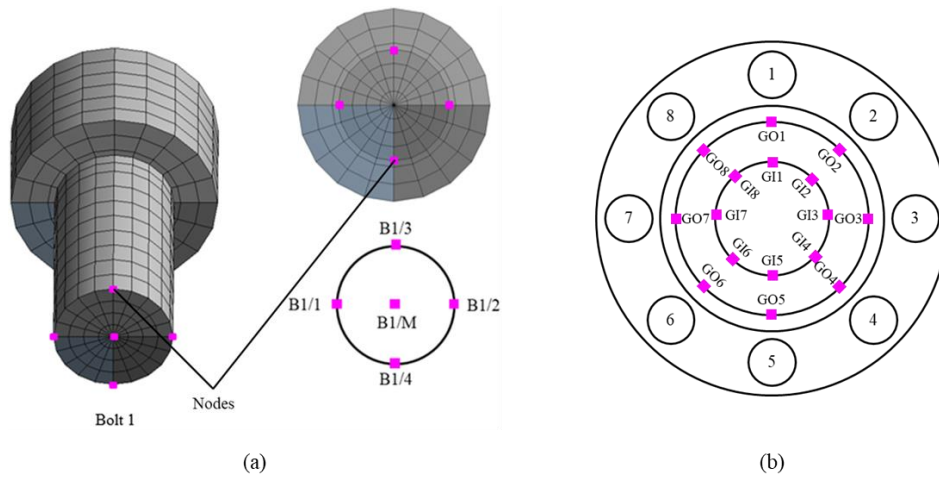


Figure 8. (a) Bolt nodes for measuring bolt stress and (b) Gasket nodes

Compressive stresses are observed to occur throughout the gasket as it is being pressed between the two flanges. Figure 11(a) exhibits the change in stress along the inner circumference of the gasket for the 4in. flange after each tightening pass. The stress in gasket is not uniform through the inner diameter of the gasket which is down to the scattering effect. Uneven bolt stress results in non-uniform gasket stress throughout the internal circumference. Gasket stress in all the nodes is seen to larger with each pass which is expected as target bolt stress also increases with every pass of the tightening sequence. Nodes GI1, GI2, and GI3 show relatively higher stresses than the other nodes in all the passes. After the last tightening pass, the stress in all nodes is greater than the minimum seating stress (69 MPa) showing that the gasket is properly seated along the inner diameter and there should not be any leakage through the inner gasket edge. The change in stress through the outer edge of the gasket for the 4in. flange is shown in Figure 11(b). Again, variable stress distribution is seen along the outer circumference of the gasket as well. It can also be observed that the outer edge of the gasket is under higher compressive stress than the inner edge which is down to the rotation of the flange as when a bolt is preloaded, the corresponding part of the flange is bent downwards and the outer boundary of the gasket experiences higher stress as compared to the inner circumference. Thus, maximum stress in gasket is through the outer edge of the gasket and it is less than the yield strength showing that the gasket is safely seated. Nodes GO1, GO2, and GO3 show relatively higher stresses in all the passes than the remaining nodes. Maximum stress occurs in the GO1 node which is about 121 MPa. Similarly, the GI6 node shows the minimum gasket stress of 90 MPa.

Gasket seating stress variation in case of 6in. flange is shown in Figure 11(c) and Figure 11(d). From both figures it is clear that the gasket stress is non-uniform and it varies through the inner and outer edge of the gasket. However, stress at all the gasket nodes is greater than the minimum seating stress of 69 MPa and less than the yield limit of 206 MPa showing that the gasket is properly and safely seated along the flange face and the joint is leak proof. The outer edge of the gasket experiences higher contact stress as compared to the inner edge due to flange rotation. Higher gasket contact stresses are seen in the 6in. flange model as compared to the 4in. flange. This may be due to higher bolt target stress in the case of 6in. flange. The minimum stress occurs in node GI9 which is about 144 MPa and the maximum stress occurs in node G02 which is about 174 MPa.

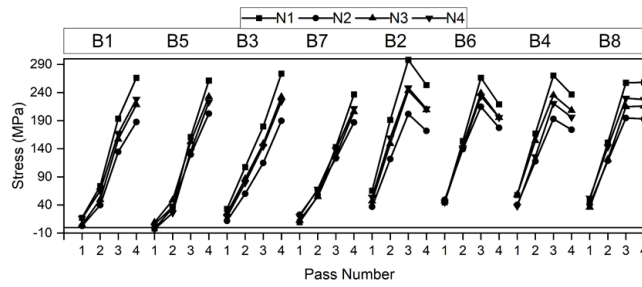


Figure 9. Bending behaviour of bolts for 4in. flange

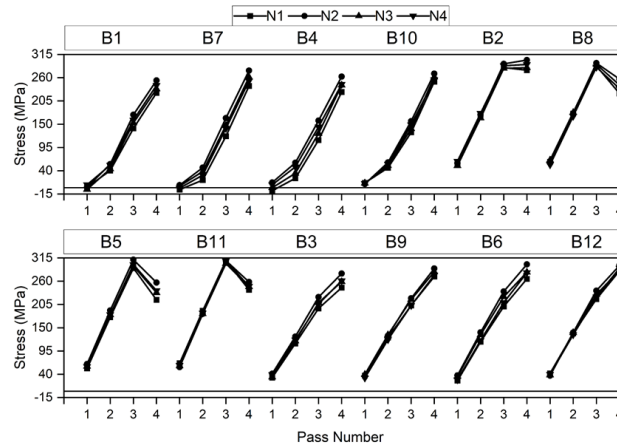


Figure 10. Bending behaviour of bolts for 6in. flange

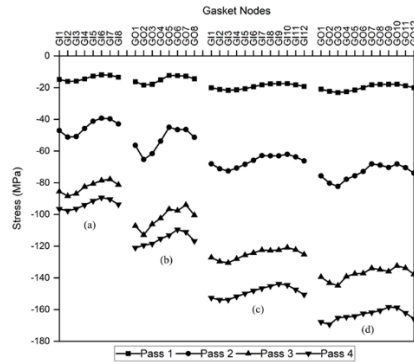


Figure 11. Gasket stress variation: (a) Inner nodes (4 in.), (b) Outer nodes (4 in.), (c) Inner nodes (6 in.), and (d) Outer nodes (6 in.)

After solving the structural model, the results of the thermal analysis are imported into the structural model to carry out an analysis of both the BFJ models under the combined action of thermal and structural loading. The thermal loading results in variation of stress in different components of the BFJ. This variation is quite prominent at high temperature. Here only the gasket stress variation is discussed as it is a fundamental factor in determining the safety of the joint. The thermal loading results in the expansion of different components of the BFJ. Due to this, relaxation in bolts is seen with greater loss in bolt stress is observed at higher bulk fluid temperatures. This loss in bolt stress also affects the gasket seating stress. Similarly, the expansion of the gasket with thermal loading also affects its sealing performance. The expansion of the gasket in the axial direction results in better sealing capability while the radial expansion decreases the gasket stress making the joint susceptible to leakage failure. To make sure that the BFJ is still operating safely at higher temperatures, it is necessary to determine the variation of gasket stress with thermal loading.

Figure 12 shows the transient behaviour of gasket inner nodes' stress with bulk fluid temperature. The variation of stress with temperature is minimal at 100 °C with an average reduction of around 7.5% is observed. As the bulk temperature is increased, stress variation also becomes more prominent. Initially, an increase in gasket stress is observed. However, as time passes, gasket stress starts to decrease and follows the same trend up to the steady-state point. At 200 °C, around 20% of gasket stress is relaxed. But the stress in all the inner nodes remains greater than the minimum seating stress (68 MPa). As the temperature is further increased, gasket stress becomes less than the minimum requirement implying possible leakage of the joint. At 300 °C, stress relaxation up to 30% is observed. Only GI2 and GI3 nodes have

stress greater than the minimum target stress at 300 °C. All other nodes have relaxed below the minimum requirement. Similarly, at 400 °C, gasket stress is further reduced, and all the inner nodes have relaxed below the minimum limit (68 MPa) implying that the gasket becomes completely relaxed along the inner circumference when bulk fluid temperature is 400 °C. The minimum stress at 400 °C occurs in the GI6 node which is 49.5 MPa as compared to the initial stress value of 89.5 MPa. This shows a reduction in stress of about 45% (40 MPa). Similarly, the maximum stress occurs in the GI2 node which is about 56.5 MPa as compared to the initial value of around 98 MPa. Thus, stress in the GI2 node is reduced by 42% (41.5 MPa).

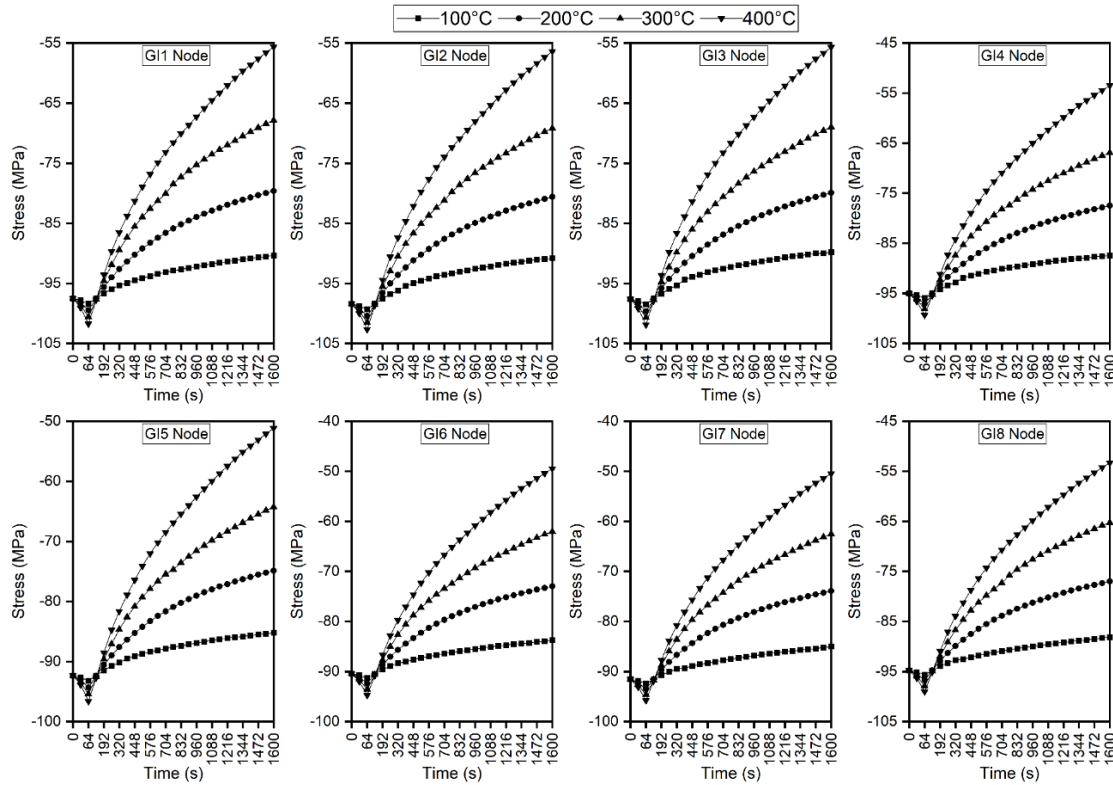


Figure 12. Gasket stress variation with temperature along inner nodes (4 in. model)

The behaviour of stress along the outer gasket nodes for the case of 4in. flange is shown in Figure 13. The stress variation is similar to that of inner nodes. Variation is smaller at 100 °C and becomes greater as the bulk temperature is raised further. At 100 °C, an average stress reduction of around 5% is observed in outer gasket nodes. Similarly, at 200 °C, this value increases to around 11%. At 300 °C, the stress in outer gasket nodes becomes further relaxed to about 18% of the initial value. At 400 °C, this stress relaxation increases to about 25% of the initial stress value. Despite this greater relaxation, the stress in all the outer gasket nodes remains higher than the minimum requirement showing that the outer edge of the gasket remains properly seated. The minimum stress at 400 °C is in the GO6 node which is about 82 MPa as compared to the initial value of 111 MPa. Thus, stress relaxation of around 26% (29 MPa) occurs in the GO6 node at 400 °C. Similarly, the maximum stress of 94 MPa is observed in the GO2 node at 400 °C as opposed to the initial value of 124 MPa. Thus, relaxation of about 24% (30 MPa) occurs in the GO2 node.

The transient behaviour of the gasket stress along the inner nodes for 6in. flange model is given in Figure 14. A large decrease in gasket stress is observed for all the nodes. However minimum stress at all the inner nodes remains greater than the minimum seating stress of 68 MPa even at high temperatures. At 100 °C, an average stress reduction of around 7.5% is seen in the inner gasket nodes. Similarly, at 200 °C, around 20% relaxation in gasket stress is observed which further increases to about 32% at 300 °C. At 400 °C, even greater loss in gasket stress is observed with average stress relaxation of around 45% can be seen in the gasket inner nodes. The minimum stress of 78 MPa is observed in the GI9 node at 400 °C. The initial stress value of the GI9 node is about 145 MPa. Thus at 400 °C, the gasket stress at the GI9 node becomes relaxed by 67 MPa which is about 46% of the initial value. However, this stress is still greater than the minimum requirement showing that the inner edge of the 6in. flange gasket remains properly seated even at a higher bulk fluid temperature of 400 °C.

Similar stress variation is also observed along the outer gasket nodes for 6in. flange as shown in Figure 15. At 100 °C, minimal relaxation is seen with an average stress variation of around 4%. Similarly, at 200 °C, around 10% reduction in gasket stress occurs which further increases to about 16% at 300 °C. At 400 °C, greater relaxation is observed, and the gasket stress is reduced by 24% of the initial value. At 400 °C, the minimum stress of 121 MPa occurs in the GO9 node which is about 75% of the initial stress value. Thus, the gasket stress remains within the acceptable limit for the case of 6in. flange, emphasizing the viability of 6in. flange joint for high temperature applications as compared to the 4in. flange joint.

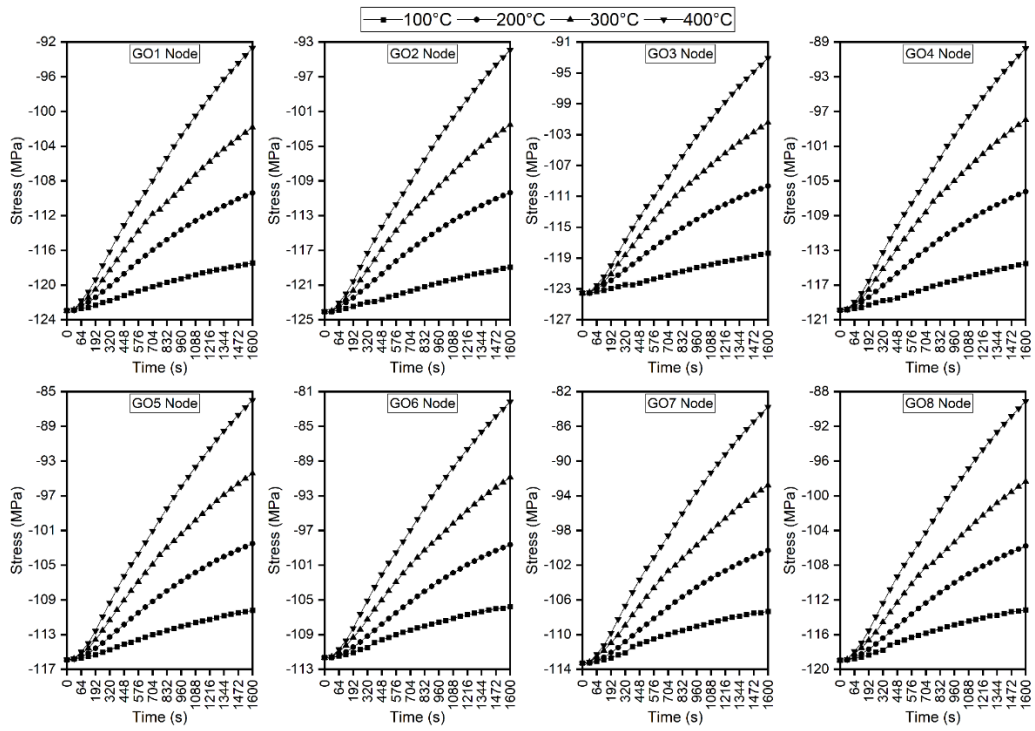


Figure 13. Gasket stress variation with temperature along outer nodes (4 in. model)

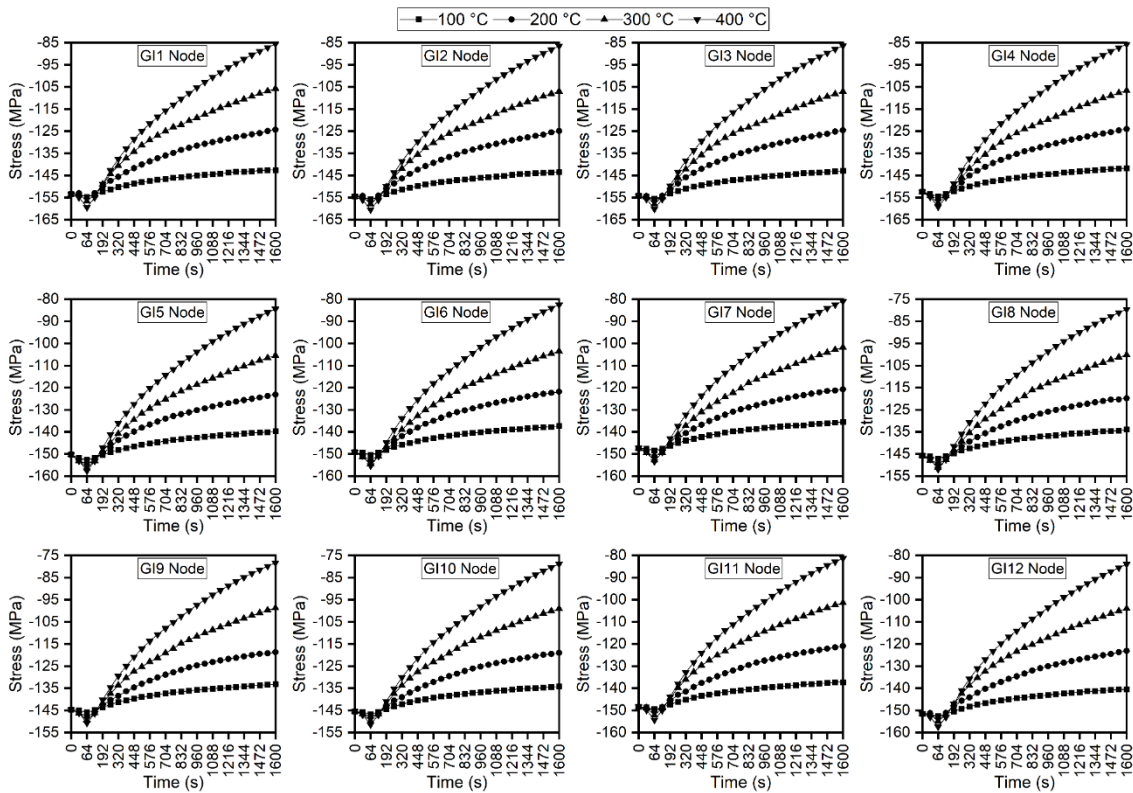


Figure 14. Gasket stress variation with temperature along inner nodes (6 in. model)

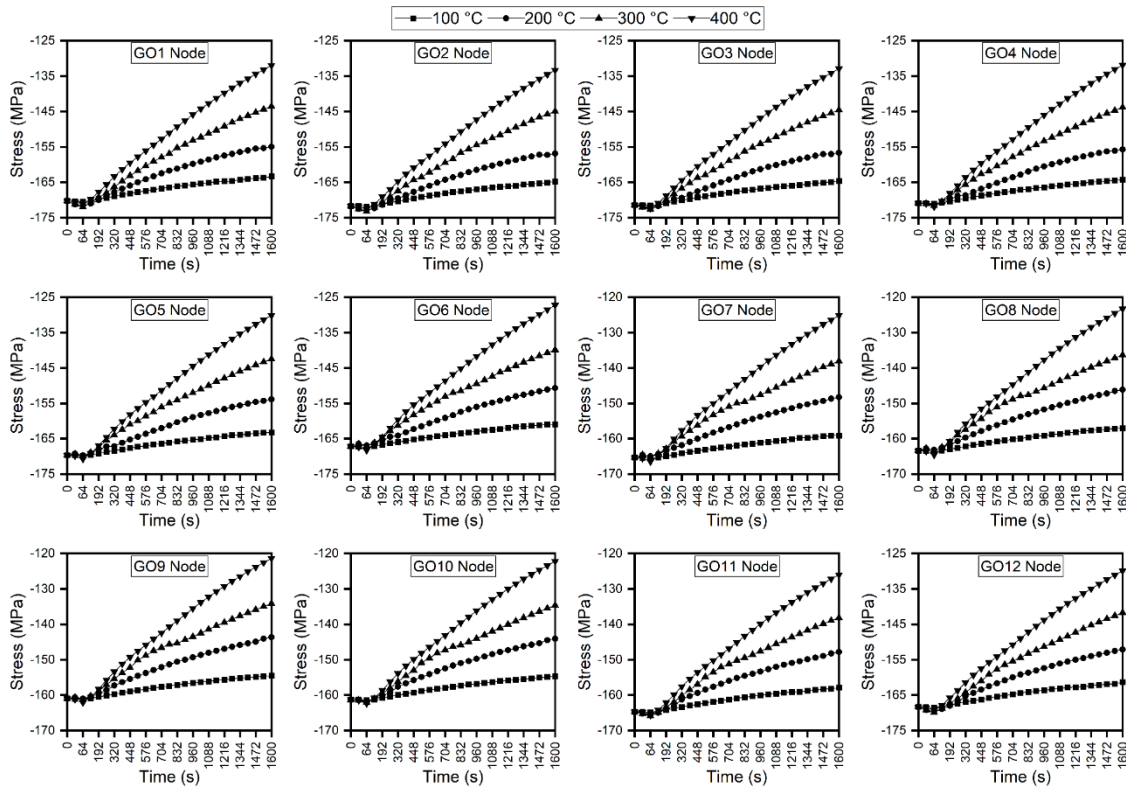


Figure 15. Gasket stress variation with temperature along outer nodes (6in. model)

4.0 CONCLUSION

The above study can be concluded as follows:

- 1) Due to scattering phenomena, non-uniform bolt stresses are observed in both flange sizes. Greater bolt stress variation is observed in the case of 6in. flange which may be down to the higher number of bolts.
- 2) In both flange models under structural loading, the gasket stresses are greater than the minimum seating stress and less than the yield limit. Also, maximum stress is observed through the outer gasket edge which is down to the rotation of the flange.
- 3) The thermal loading greatly affects the performance of GBFJ. Due to high temperature, expansion of different components is observed which results in relaxation of the joint. At lower temperature, the effect is minimal. However, as the temperature is increased, it results in greater stress relaxation in both BFJ models.
- 4) In 4 in. flange, the minimum gasket stress along the inner nodes becomes less than the minimum required stress (68 MPa) at 300 °C. However, in the case of 6in. flange, the minimum gasket stress is found to be still greater than the minimum requirement even up to 400 °C. Thus, the 6 in. model is found to be more suitable for applications where the BFJ is subjected to high temperatures as compared to the 4in. model.

5.0 REFERENCES

- [1] L. de la Roca, I. Meira, C. D. Girão, and J. Carlos Veiga, "Numerical approaches for bolt interactions in flange gasket assemblies," in *ASME Pressure Vessels and Piping Conference*, vol. 86151, p. V002T02A007, 2022.
- [2] A.-H. Bouzid and M. Derenne, "Analytical modeling of the contact stress with nonlinear gaskets," *Journal of Pressure Vessel Technology*, vol. 124, no. 1, pp. 47-53, 2002.
- [3] T. Fukuoka and T. Takaki, "Finite element simulation of bolt-up process of pipe flange connections with spiral wound gasket," *Journal of Pressure Vessel Technology*, vol. 125, no. 4, pp. 371-378, 2003.
- [4] A. Nechache and A.-H. Bouzid, "The determination of load changes in bolted gasketed joints subjected to elevated temperature," in *ASME Pressure Vessels and Piping Conference*, vol. 16982, pp. 139-148, 2003,
- [5] B. Cao, C. Duan, and H. Xu, "3-D finite element analysis of bolted flange joint considering gasket nonlinearity," *Journal-Beijing University of Chemical Technology*, vol. 26, pp. 51-55, 1999.
- [6] S. Nagata, Y. Shoji, and T. Sawa, "A simplified modeling of gasket stress-strain curve for FEM analysis in bolted flange joint design," in *ASME Pressure Vessels and Piping Conference*, vol. 19442, pp. 53-58, 2002,

- [7] M. Abid and D. Nash, "Comparative study of the behaviour of conventional gasketed and compact non-gasketed flanged pipe joints under bolt up and operating conditions," *International Journal of Pressure Vessels and Piping*, vol. 80, no. 12, pp. 831-841, 2003.
- [8] M. Abid and D. Nash, "Structural strength: gasketed vs non-gasketed flange joint under bolt up and operating condition," *International Journal of Solids and Structures*, vol. 43, no. 14-15, pp. 4616-4629, 2006.
- [9] K. Khan, M. Abid, and J. Chattha, "Gasketed bolted flange joint's relaxation behaviour under different bolt up strategy," *Proceedings of the Institution of Mechanical Engineers, Part E: Journal of Process Mechanical Engineering*, vol. 223, no. 4, pp. 259-263, 2009.
- [10] N. B. Khan, M. Abid, M. Jameel, and H. A. Wajid, "Joint strength of gasketed bolted pipe flange joint under combined internal pressure plus axial load with different (industrial and ASME) bolt-up strategy," *Proceedings of the Institution of Mechanical Engineers, Part E: Journal of Process Mechanical Engineering*, vol. 231, no. 3, pp. 555-564, 2017.
- [11] M. Abid and N. B. Khan, "Behavior of gasketed bolted pipe flange joint under combined internal pressure, axial, and bending load: three-dimensional numerical study," *Proceedings of the institution of mechanical engineers, Part E: Journal of process mechanical engineering*, vol. 232, no. 3, pp. 314-322, 2018.
- [12] N. Rino Nelson, N. Siva Prasad, and A. Sekhar, "A study on the behavior of single-and twin-gasketed flange joint under external bending load," *Journal of Pressure Vessel Technology*, vol. 139, no. 5, p. 051204, 2017.
- [13] M. Abid, K. A. Khan, and J. A. Chattha, "Performance of a flange joint using different gaskets under combined internal pressure and thermal loading," in *Advanced Design and Manufacture to Gain a Competitive Edge: New Manufacturing Techniques and their Role in Improving Enterprise Performance*, pp. 855-864, 2008: Springer.
- [14] L. Wang, X. Chen, Z. Fan, and J. Xue, "Fem stress analysis of bolted flange joints in elevated temperature service condition," in *ASME Pressure Vessels and Piping Conference*, vol. 51616, p. V002T02A019, 2018.
- [15] N. Rino Nelson, N. Siva Prasad, and A. Sekhar, "Effect of thermal loading on sealing behavior of single and twin-gasketed flange joints," *Proceedings of the Institution of Mechanical Engineers, Part E: Journal of Process Mechanical Engineering*, vol. 230, no. 6, pp. 464-473, 2016.
- [16] *B16.5 Pipe Flanges and Flanged Fittings*, ASME, USA, 1998.
- [17] *Boiler and Pressure Vessel Code (BPVC), Section VIII, Division I*, ASME, New York, USA, 2004.
- [18] J. Spence, D. Macfarlane, and A. Tooth, "Metal-to-metal full face taper-hub flanges: finite element model evaluation and preliminary plastic analysis results," *Proceedings of the Institution of Mechanical Engineers, Part E: Journal of Process Mechanical Engineering*, vol. 212, no. 2, pp. 57-69, 1998.
- [19] A.-H. Bouzid, A. Nechache, and W. Brown, "The effect of steady state thermal loading on the deflections of a flanged joint with a cover plate," in *ASME Pressure Vessels and Piping Conference*, 2002, vol. 19442, pp. 153-162.
- [20] J. Spence and A. S. Tooth, *Pressure Vessel Design: Concepts and Principles*. CRC Press, 2012.
- [21] ASME Standard, "Guidelines for pressure boundary bolted flange joint assembly: PCC -1," *The American Society of Mechanical Engineers*, United States, 2022.
- [22] "Garlock Gasket Manufacturer." Available: <http://www.garlock.com>, Accessed: February 2023
- [23] Y. Cengel, *Heat Transfer; A Practical Approach*. New York, NY, USA: McGraw-Hill, 2003.
- [24] M. Abid, D. H. Nash, S. Javed, and H. A. Wajid, "Performance of a gasketed joint under bolt up and combined pressure, axial and thermal loading–FEA study," *International Journal of Pressure Vessels and Piping*, vol. 168, pp. 166-173, 2018.
- [25] ASME BPVC, "Rules for bolted flange connections with ring type gaskets," *American Society of Mechanical Engineers: Boiler & Pressure Vessels Code, Sec. VIII, Div. I*, vol. 1, United States, 1989.